Fourth International Symposium on Marine Propulsors
smp'15, Austin, Texas, USA, June 2015

Mechanism about Change of Pressure Fluctuation of Marine Propeller Running in Bubbly Flow

Chiharu Kawakita

Mitsubishi Heavy Industries, Ltd., Nagasaki, Japan

ABSTRACT

Air lubrication system is beginning to be mounted on ships as frictional drag reduction device for ships. Air lubrication system to reduce the frictional resistance is covered by air bubbles around the hull. When an air lubrication system is applied to a ship, it is expected that the air bubbles which flowed through the circumference of a hull flow into a propeller, and it is known for the knowledge from the model experiment which made air bubbles flow into a model propeller that there is a risk of efficiency loss and an increase/decrease in the pressure fluctuations. It turns out that it is because the propeller efficiency loss is concentrated on the low pressure area of the leading edge of wing of air bubbles by a pressure gradient. However, the cause about an increase/decrease of pressure fluctuation of propeller is not clarified.

This study showed that the pressure fluctuation of propeller increases/decreases by the distribution (void fraction, air bubble layer thickness, etc.) of the bubbly flow around a propeller by using the pressure propagation analysis in bubbly flow. The mechanism of this increase/decrease is interference influence of a pressure wave, and the pressure wave in an air bubble layer is refracted and becomes close to a plane wave. By the present air lubrication system, the risk of the increase in the pressure fluctuation of propeller is high. However, the risk of increase of pressure fluctuation of propeller which is a demerit of the ship with an air lubrication system may be changed into the merit of reduction of pressure fluctuation of propeller by controlling the distribution of void fraction around a propeller.

Keywords

Air Lubrication System, Bubble Flow, Pressure Fluctuation, Bubble Dynamics

1 INTRODUCTION

The development of energy-saving ships is greatly anticipated by the shipping industry as a countermeasure against the surging prices of resources including oil, and environmental issues such as CO_2 emission regulations for international shipping operations. The air lubrication method, which reduces frictional drag by mixing air bubbles of millimeter order into the flow around the hull, has attracted attention because it can be expected to result in an especially significant energy-saving effect among other energy-saving technologies.

In April 2010, Mitsubishi Heavy Industries (hereafter MHI) completed Yamatai as shown in Fig. 1, a module carrier ordered by NYK-Hinode Line, Ltd., which was the world's first newly built ship equipped with the Mitsubishi Air Lubrication System (hereafter MALS) advanced air lubrication method. Fig. 2 shows a conceptual image of a ship equipped with MALS. The ship achieved an energy-

Figure 1: The world's first newly built ship with MALS.

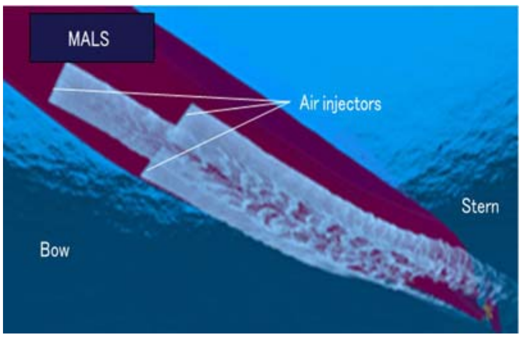

Figure 2: Image of ship equipped with MALS. The bottom of the ship is covered by air bubbles released from the air injectors.

saving effect of more than 10% attributable to MALS during actual ship tests in a sea trial (Mizokami et al. 2010). In December 2010, MHI completed Yamato, Yamatai's sister ship, which was also equipped with MALS. Using Yamato, the energy-saving effect was verified in a sea trial, the flow of air bubbles around the ship bottom was observed with a towed underwater vehicle as shown in Fig. 3, and the local frictional drag was measured by shear stress sensors installed on the bottom of the ship. As a result, actual ship data valuable for the enhancement of the frictional drag reduction effect of MALS were acquired. As five years have elapsed since the module carrier went into service, MALS is still working without any major failures. MHI is now aiming at expanding MALS to ferries, bulk carriers, and large passenger ships (Mizokami et al. 2013).

This study showed that the pressure fluctuation of propeller increases/decreases by the distribution (void fraction, air bubble layer thickness, etc.) of the bubbly flow around a propeller by using the pressure propagation analysis in bubbly flow. The mechanism of this increase/decrease is interference influence of a pressure wave, and the pressure wave in an air bubble layer is refracted and becomes close to a plane wave.

By the present air lubrication system, the risk of the increase in the pressure fluctuation of propeller is high. However, the risk of increase of pressure fluctuation of propeller which is a demerit of the ship with an air lubrication system may be changed into the merit of reduction of pressure fluctuation of propeller by controlling the distribution of void fraction around a propeller.

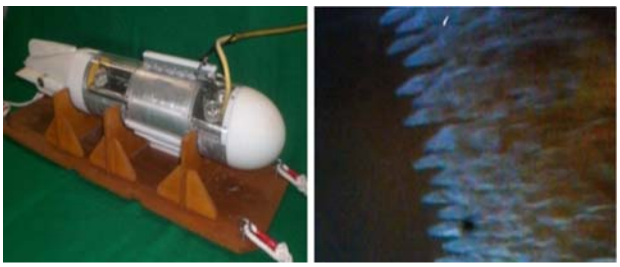

Figure 3: Towed underwater vehicle containing a camera (left photograph) and air bubble flow released from air injector of actual ship (right photograph).

2 FLOWCHART OF ENERGY-SAVING EFFECT PREDICTION ATTRIBUTABLE TO MALS

Although the propulsive power of a typical ship is estimated from the results of a tank test using a model ship, it is difficult to estimate the propulsive power of a ship equipped with MALS in this manner. This is because it is necessary to facilitate the flow of air bubbles of micrometer order around the model ship hull (compared with air bubbles of millimeter order around an actual ship) according to the model size, which is difficult to do by simple blowing air from the model ship. Therefore the tank test, for which there is no choice but to use air bubbles larger than the scale ratio of the model, results in the underestimation of the frictional drag reduction effect and air bubble distribution around the propeller. For this reason, it is necessary and important for the estimation of the energy-saving effect of a ship equipped with MALS to use a prediction technology that combines a tank test and a CFD-based prediction method of the frictional drag reduction effect (Kawakita 2014).

Fig. 4 shows the assumed flow of the energy-saving effect attributable to MALS. First, the air injector location and the amount of air blow-off volume are set, and then the air bubble distribution (void fraction distribution) around the hull and the propeller is estimated using the results of CFD-based simulation of the air bubble flow around the hull. Next, data of the void fraction distribution in the vicinity of the hull surface is input and the simulation of the reduction in frictional drag is performed using MHI's proprietary frictional drag reduction model. With reference to the void fraction distribution at the location of the propeller acquired from the simulation of the air bubble flow around the hull, the efficiency of the propeller in the bubbly flow and the change in the propeller pressure fluctuation that is necessary for the prediction of hull vibration are estimated using a combination of experiments and simulation.

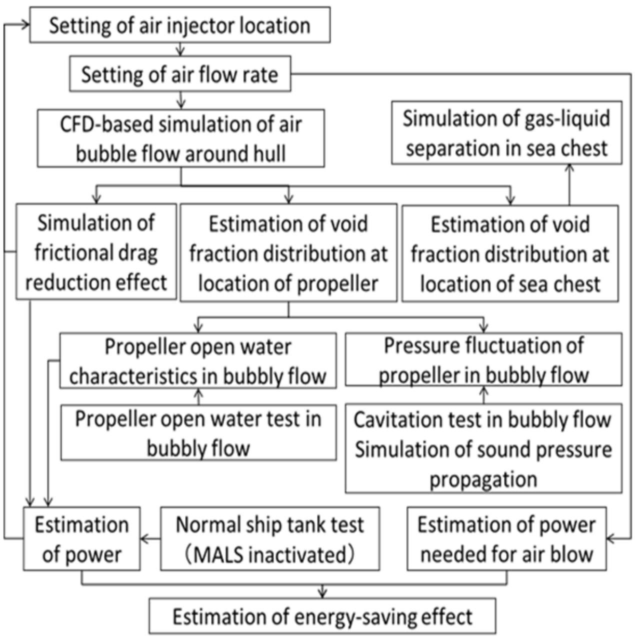

Figure 4: Flowchart of energy-saving effect prediction attributable to MALS.

In the examination of MALS, the increase/decrease of the pressure fluctuation of the propeller affected by the air bubbles is predicted through simulation technology for sound pressure propagation using the finite element method and the cavitation test in bubbly flow with the model propeller shown in Fig. 5 (Kawakita 2013). The thickness of the air bubble layer and the void fraction distribution between the propeller and the bottom of the hull are set with reference to the void fraction distribution around the propeller obtained from the simulation of the air bubble flow around the hull. Then, the increase/decrease of the pressure fluctuation of the propeller corresponding to the propeller blade frequency is estimated using a calculation model that has a point pressure source simulating fluctuating cavitation on the propeller.

Finally, the net energy-saving effect is obtained by estimating the power needed for air blow and subtracting it from the energy-saving effect of the reduction in frictional drag. In addition, the amount of air bubbles taken into the sea chest that is an engine cooling water suction port, is estimated based on the void fraction distribution around the hull to determine the shape and internal structure that can perform gas-liquid separation successfully, based on the gas-liquid simulation in the sea chest.

For the development and design of MALS, which applies an air lubrication method that reduces frictional drag by mixing air bubbles of millimeter order into the flow around the hull, the utilization of simulation technology is essential. A CFD-based prediction technology for air bubble distribution around a hull and a prediction technology for the frictional drag reduction effect using MHI's own frictional drag reduction model are key technologies for the estimation of the energy-saving effect of MALS.

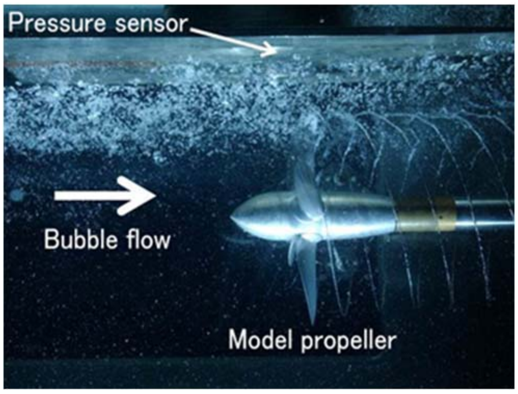

Figure 5: Cavitation test in bubbly flow. The propeller pressure fluctuation was measured by multiple pressure sensors embedded in the measuring plate immediately above the propeller. Air bubbles flowed from the air bubble release device installed on the upstream side.

3 THE PREDICTION METHOD OF INCREASE/ DECREASE OF AN EFFECT OF PROPELLER PRESSURE FLUCTUATION BY AIR BUBBLES

3.1 The Theory of Linear Pressure Waves in Bubbly Liquids

3.1.1 Underwater Acoustic Velocity Containing Air Bubbles

The underwater sound speed containing air bubbles is represented by the complex sound speed C_m of the following formula using the underwater sound speed C in the clear liquid.

$$C_m = C \Big/ \sqrt{1 + 4\pi C^2 \frac{nr}{\omega_0^2 - \omega^2 + 2ib\omega}} \tag{1}$$

where r is the bubble radius, n is the bubble number per unit volume, ω is the angular frequency, ω_0 is the natural frequency of air bubbles, b is the damping constant by the motion of air bubbles, the thermal diffusion and the sound radiation.

3.1.2 Increase and Decrease Effect of Sound Waves by Air Bubbles

The reduction of the sound waves $TL(dB)$ go through the air bubble layer is represented by the following equation.

$$TL = 20 \log \left(\frac{\exp(iks)}{\cos k_m s + \frac{i}{2}\left(\frac{C}{C_m} + \frac{C_m}{C} \right) \sin k_m s} \right) , \tag{2}$$

where s is the thickness of air bubbles layer and the wave number in the mixture k_m is given by

$$k_m = \omega / C_m \, . \tag{3}$$

3.2 THREE-DIMENSIONAL NUMERICAL ANALYSIS OF PRESSURE WAVES IN BUBBLY LIQUIDS

3.2.1 Three-Dimensional Numerical Analysis of Two-Phase Fluid Sound Pressure Propagation

Fundamental equation of acoustic pressure propagation analysis in gas-liquid two-phase flow is the wave equation (6) which is obtained from the continuity equation (4) and the momentum conservation equation (5) .

$$\frac{1}{\rho C^2}\frac{\partial P}{\partial t} + \nabla \cdot \boldsymbol{u} = \frac{\partial \alpha}{\partial t}, \tag{4}$$

$$\rho \frac{\partial \boldsymbol{u}}{\partial t} + \nabla \boldsymbol{P} = 0 \, , \tag{5}$$

$$\frac{1}{C^2}\frac{\partial^2 P}{\partial t^2} - \nabla^2 P = \rho\frac{\partial^2 \alpha}{\partial t^2}, \quad (6)$$

where t and ρ denote the time and the local mixture density. P and $\boldsymbol{u}$ indicate the average pressure and velocity. α is the local fraction of volume occupied by air (hereafter void fraction) given by

$$\alpha = \frac{4}{3}\pi r^3 n\,. \quad (7)$$

The three-dimensional numerical analysis for the wave equation carried out with a sound field 3D-FEM model by setting the density of mixture and the complex sound velocity expressed by equation (1).

3.2.2 Verification of Numerical Analysis

In order to confirm that it is possible to analyze the propagation of sound waves in bubbly flow by 3D-FEM, it is confirmed the calculation accuracy by creating an experimental model shown in Fig. 6 that is equal to the experiments described in Commander and Prosperetti (1989). Comparison of experimental results and calculation results about two cases of α=0.0337%, r=0.994mm and α=1.0%, r=2.68mm are shown in Fig. 7, where α is the average void fraction in air bubble layer and r is the bubble radius. The calculation results of the sound pressure reduction effect almost consistent with an experimental results in more than 100Hz of frequency, and it is consider that the analysis method is reasonable.

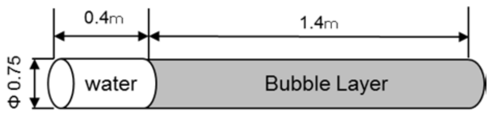

Figure 6: Calculation Model.

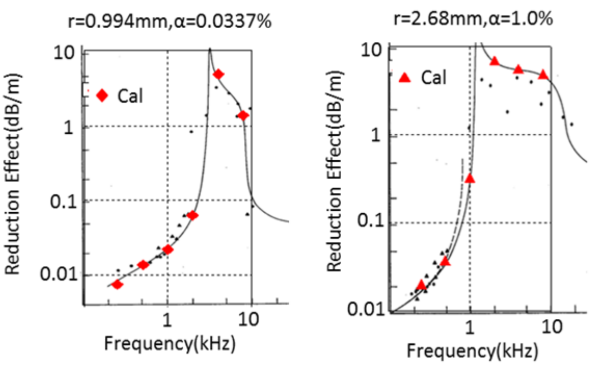

Figure 7: Comparison of reduction effect of sound pressure between calculation and experiment from Commander and Prosperetti (1989).

4 The INCREASE/DECREASE OF PROPELLER PRESSURE FLUCTUATION BY AIR BUBBLES

The air bubbles flowing around the hull are anticipated to flow into the propeller when a ship is equipped with MALS. Based on knowledge acquired from a tank test, it is known to lead to a decrease in efficiency of the propeller and increase/decrease in the pressure fluctuation of the propeller. An accumulation of air bubbles at the leading edge because of the pressure gradient contributes to the decrease in the efficiency of the propeller (Kawamura et al. 2007). On the other hand, it is becoming clear that the increase/decrease in the pressure fluctuation of the propeller is affected by the reflection, interference, and other phenomena of pressure waves at the air bubble layer between the propeller and the bottom of the hull.

4.1 The Increase/Decrease Effect in Uniform Void Fraction

One-dimensional theory (1D-theory) shown in Chapter 3 and three-dimensional numerical analysis (3D-FEM) were carried out to the computational model in which a point pressure source that simulated a fluctuating cavity at the tip of a propeller shown in Fig. 8. In the calculations, the air bubble layer with uniform void fraction was set between the propeller and the bottom of the hull. In the case of changing the air bubble layer thickness BL and bubble radius r, the increase/decrease of pressure fluctuations $\Delta P/\Delta P_0$ corresponding to each blade frequency were calculated.

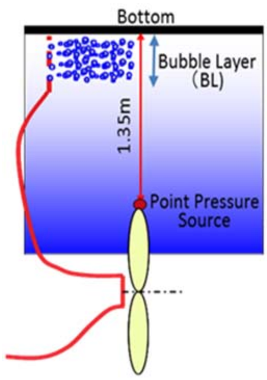

Figure 8: Calculation model for pressure fluctuation of propeller.

(1) 1D-theory

One-dimensional theoretical solution of the reduction effect of the pressure fluctuation in the bubble radius r=0.5mm and the air bubble layer BL=1m is shown in Fig. 9. In this condition, the pressure fluctuation decreases in any frequency, and also as the average void fraction α is high and up to a frequency of 35Hz, the reduction effect of the pressure fluctuation $\Delta P/\Delta P_0$ becomes higher.

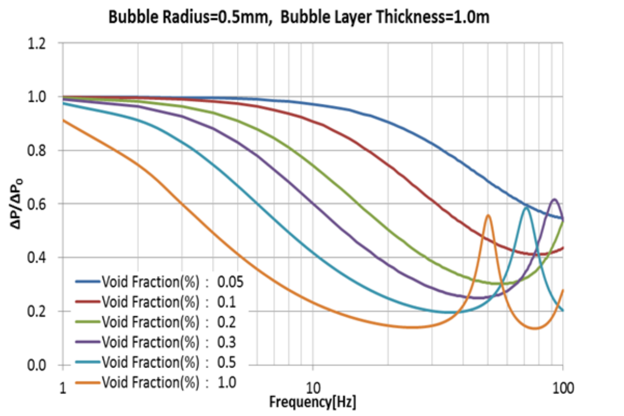

Figure 9: Comparison of reduction effect of pressure fluctuation by change of average void fraction calculated by 1D- theory (r=0.5mm, BL=1m).

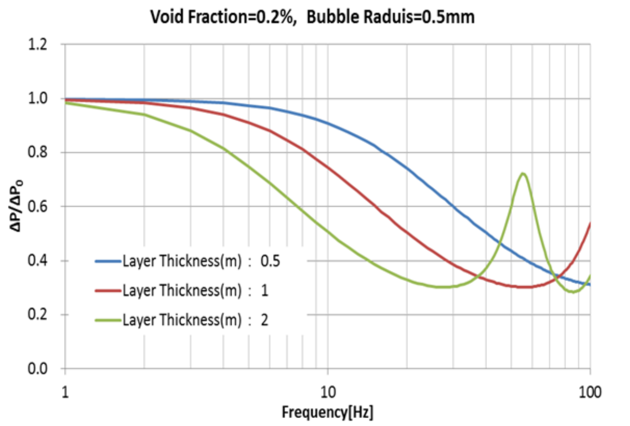

Figure 11: Comparison of reduction effect of pressure fluctuation by change of air bubble layer thickness calculated by 1D-theory (α=0.2%, r=0.5mm).

The reduction effect of the pressure fluctuation in the average void fraction is 0.2%, the air bubble layer is 0.5m and the air bubble radius is changed from 0.5mm to 10mm is shown in Fig. 10. The influence of the air bubble radius to the reduction effect of the pressure fluctuation is small.

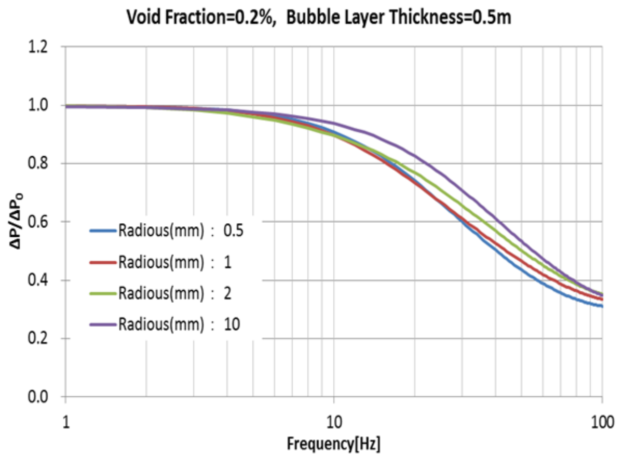

Figure 10: Comparison of reduction effect of pressure fluctuation by change of bubble radius calculated by 1D-theory (α=0.2%, BL=0.5m).

The reduction effect of the pressure fluctuation in the average void fraction is 0.2%, the bubble radius is 0.5mm and the air bubble layer is changed from 0.5m to 2.0m is shown in Fig. 11. The influence of the air bubble layer thickness to give the reduction effect of the pressure fluctuation is big. Until the frequency of 35Hz, the pressure fluctuation reduction effect is higher as the air bubble layer is thicker.

(2) 3D-FEM

Three-dimensional numerical analysis of the reduction effect of the pressure fluctuation in the bubble radius r=0.5mm and the air bubble layer BL=1m is shown in Fig.12. The results of 3D-FEM differ from the results of 1D-theory solution, it followed that the pressure fluctuation increased ($\Delta P/\Delta P0>1.0$) or decreased depending on frequency. The first blade frequency of propeller pressure fluctuation is around 10Hz. At this frequency, the pressure fluctuation increases in all average void fraction and it becomes 1.2-1.3 times in comparison with the case without air bubbles. The frequency that the pressure fluctuation decreases appears in low frequency region of around 2-4Hz and high frequency region more than 20kHz.

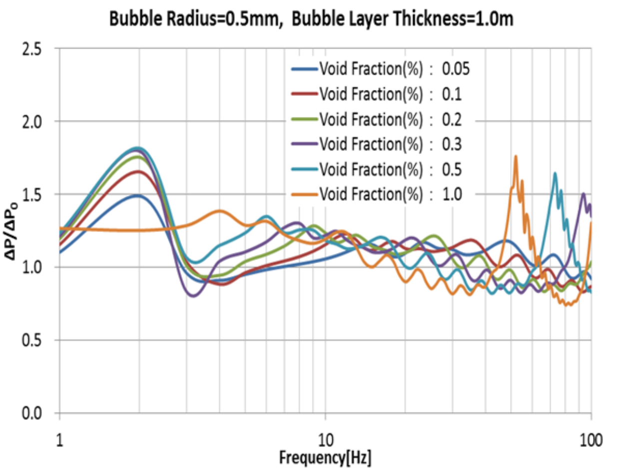

Figure 12: Comparison of reduction effect of pressure fluctuation by change of average void fraction calculated by 3D-FEM (r=0.5mm, BL=1m).

The reduction effect of the pressure fluctuation in the average void fraction 0.2%, when changing air bubble layer thickness from 0.5m to 1.0m, is shown in Fig. 13. The influence of air bubble layer thickness finds out that the pressure fluctuation has a big influence on a reduced frequency region.

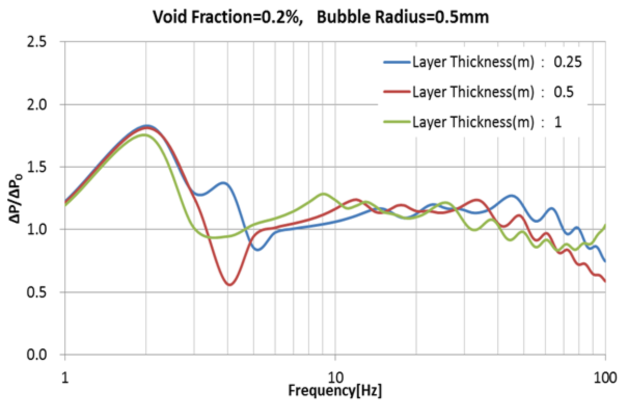

Figure 13: Comparison of reduction effect of pressure fluctuation by change of air bubble layer thickness calculated by 3D-FEM (α=0.2%, r=0.5mm).

It turned out that the increase/decrease of a tendency of pressure fluctuation differ greatly with the results of 1D-theory and 3D-FEM. Because the 1D-theory deals with a pressure wave as plane wave, it isn't possible to consider interference influence of the pressure wave by the case that the pressure wave bends by air bubble influence. Therefore, in order to evaluate accurately the increase/decrease effect of pressure fluctuation of marine propeller running in the bubbly flow, it is found that it is necessary to estimate accurately air bubble distribution between the propeller and the bottom of the hull, i.e. void fraction distribution and to carry out sound pressure propagation analysis in two phase flow by using 3D-FEM.

4.2 The Increase/Decrease Effect in Nonuniform Void Fraction

When the void fraction distribution in the air bubble layer isn't uniform and is non-uniform, the increase/decrease of pressure fluctuation distribution is investigated using three-dimensional numerical analysis (3D-FEM). Typically, the air bubble layer between the propeller and the bottom of the hull tends to have a higher void fraction when the layer is closer to the bottom of the hull. Therefore, with the average void fraction kept constant, the void fraction distribution in the air bubble layer has a higher void fraction in the vicinity of the bottom of the hull when the air bubble layer thickness is thinner. The void fraction distribution is similar by the function of square root of the air bubble layer thickness at the void fraction for uniformity at the average void fraction in reference to the bubble flow calculation around the hull as shown in Chapter 2. The two kinds of average void fraction α =2.25% and 4.5% are used for calculation. The void fraction distribution at the time of changing three kinds of air bubble layer thickness BL(1.35m, 0.675m, 0.45m) to each average void fraction is set up. Compared with 6 different void fraction distribution are shown in Fig. 14. First of all, the propeller pressure fluctuation reduction effect was researched while maintaining a constant average void fraction in the air bubble layer and changing the air bubble layer thickness. The reduction effects of the pressure fluctuation at the time of changing the air bubble layer thickness BL are shown in Fig. 15 (α=2.25%, r=0.5mm) and Fig. 16 (α=4.5%, r=0.5mm). The value higher than the general average void fraction of the air bubbles which flow into the propeller by the air lubrication method is set up. When the average void fraction α is 2.25%, the reduction effect of pressure fluctuation is not seen in 10Hz of frequency, but when a frequency is more than 20 Hz, the reduction effect of more than 20 % of pressure fluctuation is seen when air bubble layer thickness is thin. When the average void fraction α is 4.5%, the reduction effect of the pressure fluctuation shows from 10Hz of frequency, and if the air bubble layer thickness BL becomes thin, the reduction effect of more than 20% of pressure fluctuation is seen.

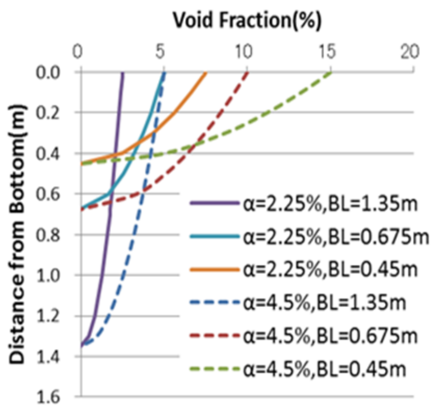

Figure 14: Distribution of void fractions used for 3D-FEM.

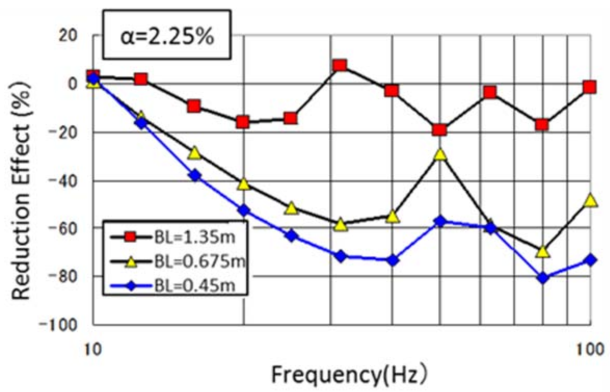

Figure 15: Comparison of reduction effect of pressure fluctuation by change of air bubble layer thickness calculated

by 3D-FEM (α=2.25%, r=0.5mm). This shows the change in the pressure fluctuation of the propeller corresponding to the change in the thickness of the air bubble layer between the propeller and the bottom of the hull and the change in the propeller blade frequency.

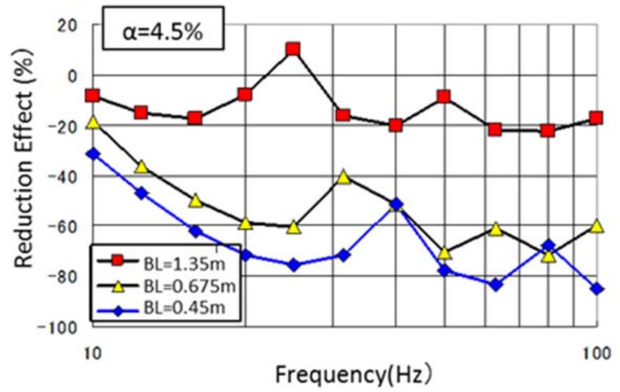

Figure 16: Comparison of reduction effect of pressure fluctuation by change of air bubble layer thickness calculated by 3D-FEM (α=4.5%, r=0.5mm).

These results represent no pressure fluctuation reduction effect in the lower frequency region. In the higher frequency region, however, the thinner the air bubble layer thickness becomes, the more the pressure fluctuation reduction effect increases. For this reason, the condition for reducing the propeller pressure fluctuation is regarded as the establishment of a thin air bubble layer with a high void fraction in the vicinity of the bottom of the hull.
Assuming the development of a technology for controlling void fraction distribution at the location of the propeller, the disadvantageous risk of increasing propeller pressure fluctuation in a ship equipped with MALS might become the advantage of reducing the pressure fluctuation of a propeller. Such technologies include controlling the air bubble flow by providing new air bubble flow in the vicinity of the bottom of the hull from the upstream of the propeller or by collecting air bubbles flowing along the bottom of the hull in front of the propeller and releasing them again in the vicinity of the bottom of the hull on the upstream side of the propeller.
For the study of a mechanism that increases the pressure fluctuation of a propeller, Fig. 17 shows the pressure fluctuation distributions for cases where an air bubble layer exists and where no air bubble layer (only water) exists, together with the air bubble layer thickness and the frequency which lead to the increase in the pressure fluctuation (It corresponds to the air bubble layer thickness BL=1.35m and the frequency=31.5Hz in Fig. 15). In cases where the air bubble layer exists, the propeller pressure fluctuation at the bottom of the hull decreases due to the reflection of pressure waves at the boundary of the air bubble layer and the pressure damping effect in the air bubble layer. However, the standing wave (antinode-node-antinode) occurs in the direction of the air bubble layer thickness due to the interference of pressure waves in the air bubble layer and therefore the propeller pressure fluctuation at the bottom of the hull increases at the frequency where the standing wave occurs.

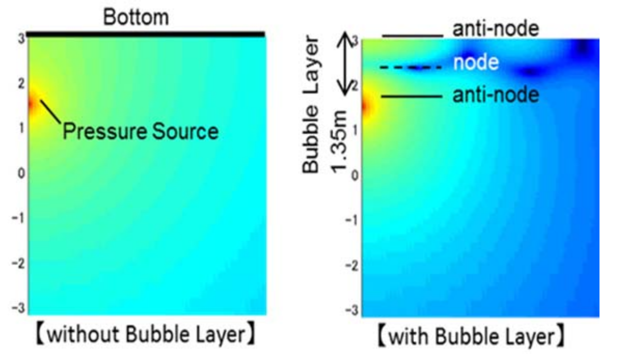

Figure 17: Change in pressure fluctuation distribution with and without air bubble layer at 31.5Hz (r=0.5mm, BL=1.35m). These are contour figures of the distributions of the pressure fluctuation propagating from the pressure source (red area) where the pressure fluctuation is high.

The air bubble layer thickness BL shall be 0.45 m, the reduction effect of the pressure fluctuation at the time of changing the average void fraction from 2.25% to 6% is compared as shown in Fig. 18. With the increase in the average void fraction, the pattern of the pressure fluctuation reduction effect is shifted to the low frequency region. It is thought that the pressure fluctuation reduction effect shifts to the low frequency region by the increase of the average void fraction because the acoustic speed in the air bubble layer decreases.

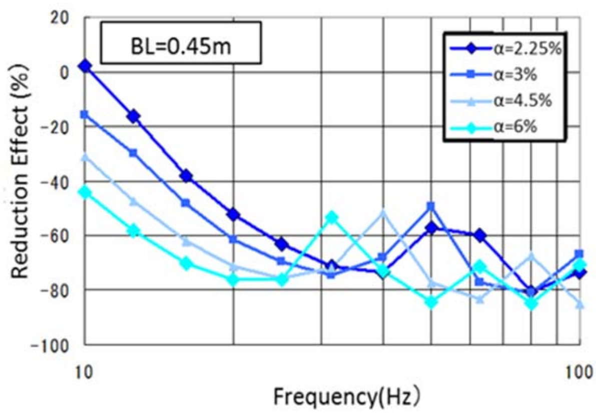

Figure 18: Comparison of reduction effect of pressure fluctuation by change of average void fraction calculated by 3D-FEM (r=0.5mm, BL=0.45m).

4.3 Consideration about the Mechanism of Pressure Fluctuation Reduction Effect Improvement in Thin Air Bubble Layer Thickness

When there is no air bubble layer (in the case only of water), the pressure wave spreads in three dimensions and it decreases with distance. On the other hand, when an air bubble layer exists, since the acoustic speed in an air bubble layer is small to the case of only water, the pressure wave from the point pressure source which is a curved-surface wave as shown in Fig. 19, is refracted and turns into a plane wave, and it becomes difficult to damp by distance. Here, the relation of the underwater sound speed C_1=1500 m/s, the underwater sound speed in bubbly flow C_2=about 100 m/s and θ_1, θ_2 can be approximated by the following formula.

$$\sin\theta_1 / \sin\theta_2 = C_1 / C_2 \ , \qquad (8)$$

$$\sin\theta_2 \cong 0 \quad \rightarrow \quad \theta_2 = 0 \qquad (9)$$

In the case where air bubble layer thickness is thin, the reason a pressure wave reduction effect is large is considered because a pressure wave is reduced in the air bubble layer, after damping by distance in the position away from the pressure source.

Although the pressure is the point pressure source in this research, the actual pressure fluctuation of propeller is generating and collapse of a cavity, and since it has a certain distribution, it is thought that the pressure wave from actual pressure source distribution is close to a plane wave, and the difference with the case of only water becomes small.

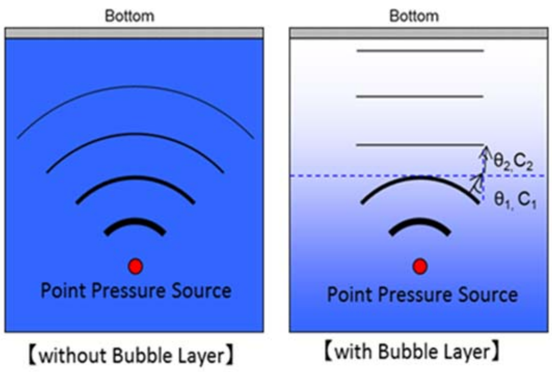

Figure 19: Comparison of pressure wave between with and without air bubble layer.

7 CONCLUSIONS AND FUTURE WORK

This study showed that the pressure fluctuation of propeller increases/decreases by the distribution of the bubbly flow around a propeller by using the pressure propagation analysis in bubbly flow. The mechanism of this increase/decrease is interference influence of a pressure wave, and the pressure wave in an air bubble layer is refracted and becomes close to a plane wave. A prediction technology for the pressure fluctuation of a propeller that rotates in the bubbly flow has the potential of turning the disadvantageous risk of increasing propeller pressure fluctuation in a ship equipped with MALS into the advantage of reducing the pressure fluctuation of a propeller. This is assuming that a technology for controlling void fraction distribution at the location of the propeller is developed in the future. Such technologies include controlling the air bubble flow by providing new air bubble flow in the vicinity of the bottom of the hull from the upstream of the propeller or by collecting air bubbles flowing along the bottom of the hull in front of the propeller and releasing them again in the vicinity of the bottom of the hull on the upstream side of the propeller.

We will continue to utilize data from actual ships equipped with MALS in simulation technologies, aiming at the enhancement of simulation accuracy, further improvement in the performance of MALS, and the expansion of ship types to which MALS is applicable.

ACKNOWLEDGMENTS

The author would like to express his sincere gratitude to Mr. Hosoya and Mr. Okimoto of the Vibration Laboratory of Nagasaki Research and Development Center, Mitsubishi Heavy Industries, Ltd., and thanks are also extended to all members of the Fluid Dynamic Laboratory for their cooperation.

REFERENCES

Commander, K. and Prosperetti, A. (1989), "Linear pressure waves in bubbly liquids: Comparison between theory and experiments," J. of Acoust. Soc. Am. 85.

Kawakita, C. (2013), "Study on Marine Propeller Running in Bubbly Flow," 3rd International Symposium on Marine Propulsors smp'13, Launceston Australia.

Kawakita, C. (2014), "Estimation of Frictional Drag Reduction Effect for the Ship with Air Lubrication System," Conference Proceedings the Japan Society of Naval Architects and Ocean Engineers (19) 2014A-JK-2

Kawamura, K., Ito, A., Hinatsu, M. (2007), "Numerical Simulation of Bubbly Flow Around a Marine Propeller," Proceedings of FEDSM2007, ASME/JSME 2007 5th Joint Fluids Engineering Conference.

Mizokami, S., Kawakita, C., Kodan, Y., Takano, S., Higasa, S. and Shigenaga, R. (2010), "Experimental Study of Air Lubrication Method and Verification of Effects on Actual Hull by Means of Sea Trial," Mitsubishi Heavy Industries Technical Review Vol.47, No.3, 41-47.

Mizokami, S. et.al. (2013), "Implementation of Ship Energy-Saving Operations with Mitsubishi Air Lubrication System," Mitsubishi Heavy Industries Technical Review, Vol.50, No.2, 44-49.